# Optical Control of Surface Anchoring and Reorientation of Liquid Crystals via a Plasmon-Enhanced Local Field

J. Shan,[1] W. Shi,[1] L. Y. Liu,[1] Y. R. Shen,[2,3] and L. Xu[1,2,*]

[1]*Key Lab for Micro and Nanophotonic Structures (Ministry of Education), Department of Optical Science and Engineering, School of Information Science and Engineering, Fudan University, Shanghai 200433, China*

[2]*Department of Physics, Fudan University, Shanghai 200433, China*

[3]*Department of Physics, University of California, Berkeley, California 94210, USA*

(Received 18 March 2012; published 2 October 2012)

Gold nanoparticles deposited on the windows of a liquid crystal (LC) cell were found to be able to reduce the surface anchoring energy of the LC, and hence the threshold for its reorientation phase transition, by 1 to 2 orders of magnitude when a cw pump light was used to excite the local plasmon resonance of the nanoparticles. The effect was due to the disorientation of LC molecules between nanoparticles by the plasmon-enhanced local field that softens the effective surface anchoring. A light-controlled variation of surface anchoring energy could provide new opportunities for optoelectronic applications of a LC.

DOI: 10.1103/PhysRevLett.109.147801 PACS numbers: 42.70.Df, 61.30.Gd, 61.30.Hn, 73.20.Mf

Optical control of liquid crystal (LC) alignment has been a subject of great interest because of its potential applications in optoelectronics. Reorientation of a LC by laser beams has been studied extensively for displays, optical switching, pattern formation, and induced nonlinear dynamics [1]. In most cases, the direct optical torque is used to reorient molecules in a LC cell. Optical excitation of LC molecules or dye molecules in a dye-doped LC can strongly enhance the torque [2–5]. In other cases, an optically induced conformation change of surfactant molecules on a substrate can render LC realignment [6–8]. So far, however, there has been no report on the optical modification of the anchoring of LC molecules at a substrate to facilitate reorientation of a LC in a cell. The anchoring of a LC is crucial for the performance of LC devices. With proper design, it can selectively align a LC parallel or perpendicular to a surface with the desired strength [9,10]. The anchoring strength, denoted by the surface anchoring energy (SAE), governs how stable LC molecules are aligned in a cell [11–13]. Higher SAE aligns the LC better, but requires a higher external field (electric, magnetic, or optical) to "switch on" a LC device [14–18]. Lowering the switching power without sacrificing SAE is often important for LC device operation. In this Letter, we report an observation that with the deposition of gold nanoparticles on a substrate, we can dynamically vary the SAE by an optical field and drastically lower the switching power, while keeping the SAE statically unchanged. The strongly enhanced local field through the local plasmon resonance between gold nanoparticles must have disoriented the LC molecules in the surface layer and caused a reduction of the effective SAE.

We briefly review here the theory behind the optical reorientation of a nematic LC. For a homeotropic LC film confined between $z = 0$ and $d$ with an $x$-polarized beam of intensity $I$ normally incident on it, the total free energy density of the system is [19]

$$f = \frac{1}{2}\left[(k_{33}\cos^2\theta + k_{11}\sin^2\theta)\left(\frac{d\theta}{dz}\right)^2\right] - \frac{I}{c}n(\theta) + \frac{1}{2}[\delta(z) + \delta(d-z)]\sum_{n=1}^{\infty} W_{2n}\sin^{2n}\theta,$$

$$n(\theta) = n_o n_e/(n_0^2\sin^2\theta + n_e^2\cos^2\theta)^{1/2}, \quad (1)$$

in which $\theta$ is the angle between the LC director and the $z$-axis, $k_{11}$ and $k_{33}$ are splay and bend elastic constants, $n_o$ and $n_e$ are ordinary and extraordinary refractive indices, and $W_{2n}$ with positive integers $n$ describes the SAE. For simplicity, we assume $W_{2n} = 0$ for $n > 2$. Equation (1) shows that at $I = I_{\text{th}}$, the LC film undergoes a second-order structural phase transition, known as the Fréedericksz transition (FT), that marks the beginning of an optical-field-induced LC reorientation. The threshold intensity $I_{\text{th}}$ is given by

$$\left(\frac{I_{\text{th}}}{I_0}\right)^{1/2}\tan\left[\frac{\pi}{2}\left(\frac{I_{\text{th}}}{I_0}\right)^{1/2}\right] = \frac{dW_2}{\pi k_{33}}, \quad (2)$$

where $I_0 = ck_{33}[n_e^2/n_0(n_e^2 - n_0^2)](\pi^2/d^2)$ is the optical FT threshold at infinite SAE [19]. A similar derivation for the magnetic-field-induced FT yields the same expression for the threshold magnetic field $H_{\text{th}}$ (parallel to the surfaces) if we replace $\sqrt{I_{\text{th}}}$ by $H_{\text{th}}$ and $\sqrt{I_0}$ by $H_0 = (\pi/d)(k_{33}/\chi_a)^{1/2}$ in Eq. (2), where $\chi_a$ is the magnetic anisotropy of the nematic LC. With the simultaneous presence of optical and magnetic fields along the same direction parallel to the surfaces, the two fields collaborate in inducing FT, leading to the following expression of $H_{\text{th}}$ for a given $I$:

$$\left[\left(\frac{H_{\text{th}}}{H_0}\right)^2 + \frac{I}{I_0}\right]^{1/2}\tan\left\{\frac{\pi}{2}\left[\left(\frac{H_{\text{th}}}{H_0}\right)^2 + \frac{I}{I_0}\right]^{1/2}\right\} = \frac{dW_2(I)}{\pi k_{33}}. \quad (3)$$

 

Here, we explicitly show that $W_2$ may depend on $I$. If $W_2(I)$ decreases with an increase of $I$, then $H_{\rm th}^2$ will decrease correspondingly in a way that is faster than linear with $I$. Equation (3) allows the determination of $W_2(I)$ from the measured $H_{\rm th}(I)$. This is the method we adopted to obtain $W_2(I)$ for our LC samples.

In our experiment, the LC material studied was 4-pentyl-4′-cyanobiphenyl (5CB). The homeotropic LC cells were prepared by using N, N-dimethyl-N-octadecyl-3-aminopro-pyltrimethoxysilyl-chloride (DMOAP) as the alignment surfactant. Gold nanoparticles were synthesized by reducing the reaction from chloroauric acid ($HAuCl_4$) and their diameter was found to be ~50 nm [20]. To prepare a nanoparticle-coated substrate, a clean optical glass plate was first dipped in the DMOAP aqueous solution for 30 min, and then immersed in the Au-nanoparticle solution for 0.5–6 h. The surface density of Au nanoparticles appearing on the plate increased with the immersion time. After the nanoparticle deposition, the substrate was again dipped in the DMOAP solution for 30 min allowing the coating of another layer of DMOAP on the Au nanoparticles to assure homeotropic LC alignment. LC cells with both windows modified this way and different cell thickness between 15 and 100 $\mu$m were prepared. Cells without a Au-nanoparticle coating on their windows were used as references.

Shown in Fig. 1(a) is an atomic force microscopy image of ~50-nm Au nanoparticles deposited on a substrate over a time period of 2 h. Figure 1(b) displays the absorption spectra of 25-$\mu$m-thick LC cells whose windows were coated by Au nanoparticles with different Au deposition times. The absorption peak near 550 nm comes from local plasmon resonance of the gold particles. Another absorption peak near 680 nm emerging at high Au-nanoparticle densities can be attributed to absorption by Au-nanoparticle clusters [21]. The threshold of FT is marked by the onset of optical birefringence arising from LC reorientation, which can be monitored by a probe beam. An example of optical FT is shown in the inset of Fig. 2(a). The main picture of Fig. 2(a) displays the measured $H_{\rm th}^2$ versus the pump intensity $I$ for a Au-LC cell that is 47 $\mu m$ thick and for reference, a pure LC cell of the same thickness. (In the experiment, the pump was a 532-nm cw beam from a frequency-doubled Nd:YAG laser, and the probe was a weak 660-nm beam from a diode laser. As seen in Fig. 1(b), the 532-nm wavelength is very close to the peak of the plasmon resonance.) We notice in Fig. 2(a) that at $I = 0$, $H_{\rm th}$ of the Au-LC cell is only slightly smaller than that of the pure LC cell, indicating that the anchoring energy of the two cells are close. Equation (3), with $n_0 = 1.54$, $n_e = 1.73$, $k_{33} = 8.5 \times 10^{-7}$ dyn, and $\chi_a = 1.2 \times 10^{-7}$ cgs for 5CB [22,23], allows us to find $W_2 = (0.75 \pm 0.11) \times 10^{-5}\ J/m^2$ and $(1.0 \pm 0.1) \times 10^{-5}\ J/m^2$, respectively, for the Au-LC and reference LC cells. In the above case, the Au deposition time in preparing the Au-LC cell was 2 h. The SAE of the Au-LC cell depends on the Au deposition time, but only weakly. Increasing the Au deposition time from 0 to 6 h changed $W_2$ at $I = 0$ from $10^{-5}$ to $0.46 \times 10^{-5}$ J/m$^2$. (See Supplemental Material [24].) As $I$ increases, $H_{\rm th}^2$ decreases, but $H_{\rm th}^2$ of the Au-LC cell decreases much faster. Note that the difference of $H_{\rm th}^2$ of the two cases at a given $I$ can reach more than 1 order of magnitude, corresponding to a significant decrease of $W_2$ of the Au-LC cell with an increase of $I$. Using the data of Fig. 2(a) and Eq. (3), we find $W_2$ versus $I$ plotted in Fig. 2(b). For the Au-LC cell, $W_2$ drops from $0.75 \times 10^{-5}$ J/m$^2$ at $I = 0$ to $(1.2 \pm 0.1) \times 10^{-7}$ J/m$^2$ at $I = 380$ W/cm$^2$ (which is the threshold intensity for the optical FT of the Au-LC cell at $H = 0$). As a comparison, $W_2 = 1.0 \times 10^{-5}$ J/m$^2$ for the pure LC cell is independent of $I$ within the experimental uncertainty. As a double check, we measured $W_2(I)$ directly using the hybrid LC cell method [25]. The hybrid LC cell had one window coated with Au nanoparticles and DMOAP for homeotropic alignment and another coated with rubbed polyimide for homogeneous alignment. The measured $W_2$ versus $I$ is also presented in Fig. 2(b), exhibiting good agreement with that deduced from the $H_{\rm th}^2(I)$ measurement.

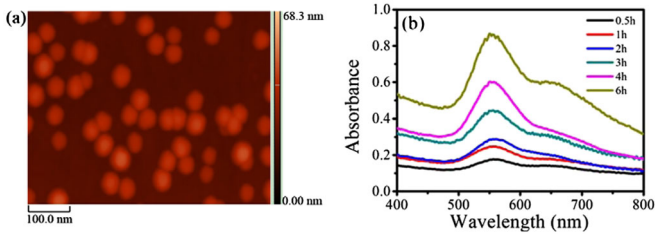


FIG. 1 (color online). (a) Atomic force microscopy image of Au nanoparticles on glass prepared by 2 h of deposition time. (b) Absorption spectra of Au-nanoparticle-coated glass prepared with various deposition times.

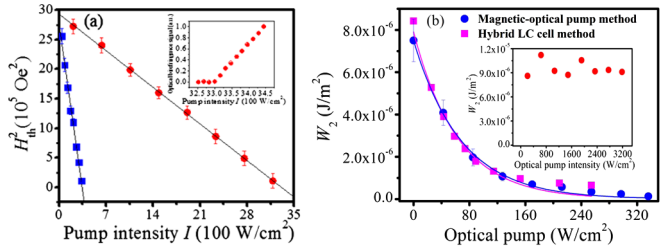


FIG. 2 (color online). (a) Measured $H_{\rm th}^2$ as a function of pump intensity $I$ for a 47 $\mu$m Au-LC cell (blue squares) and a 47 $\mu$m pure LC cell (red circles). Lines are theoretical fits. Typical error bars are shown. The inset shows the dependence of induced optical birefringence on pump intensity $I$. The onset of the optical birefringence at $I = I_{\rm th}$ marks the Fréedericksz transition. (b) $W_2$ as a function of pump intensity for the 47 $\mu$m Au-LC cell obtained from data in Fig. 2(a) and an analysis using Eq. (3) (blue circles) and by direct measurement using the hybrid cell method (magenta squares). The lines are fits with Eq. (4). Inset: $W_2$ versus $I$ for the 47 $\mu$m pure LC cell.

The reduction of $W_2$ could not come from laser heating. Absorption of the cw laser light by Au nanoparticles of the Au-LC cell could increase the temperature of the cell, but not much more than 1 °C. (See Supplemental Material [24].) Experimentally, it was found that at $I = 0$, change of $W_2$ with change of the cell temperature by 1 °C is within the error of the $W_2$ measurement.

The reduction of $W_2$ with an increase of $I$ can be qualitatively understood from the sketches in Fig. 3. Initially, the Au-LC cell has a homeotropic boundary condition for homeotropic LC alignment in the bulk. If, however, the homeotropic boundary condition is relaxed by having part of the LC molecules at the boundary surfaces tilted away from the surface normal, the effective SAE will decrease and so will the threshold of Fréedericksz transition. In the case of a Au-LC cell, LC molecules in the effective surface layer (shaded in Fig. 3) can be reoriented by an optical field much weaker than that required to reorient the LC homeotropic alignment of the bulk because of the strong local-field enhancement in the neighborhood of the Au nanoparticles. A crude estimate shows that in our case, with 50-nm Au nanoparticles, the field enhancement is ~30. An energy argument based on the known elastic constants of 5CB suggests that to reorient a 50-nm surface layer of a nematic LC by 5° in the presence of local-field enhancement only requires a light intensity of ~200 W/cm$^2$. The small tilt of surface LC molecules away from the surface normal helps reduce the FT threshold significantly.

We can fit the data of $W_2$ versus $I$ in Fig. 2(b) quite well with the expression

$$W_2(I) = W_0 e^{-I/I_{\text{sat}}}. \quad (4)$$

The values of $W_0$ and $I_{\text{sat}}$ deduced from the fit are $(0.75 \pm 0.11) \times 10^{-5}$ J/m$^2$ and $75 \pm 10$ W/cm$^2$, respectively. The expression shows that the dependence of $W_2$ on $I$ saturates at large $I$ as one would expect from the optically induced reorientation of surface LC molecules, although quantitatively, why it has the exponential dependence is not clear.

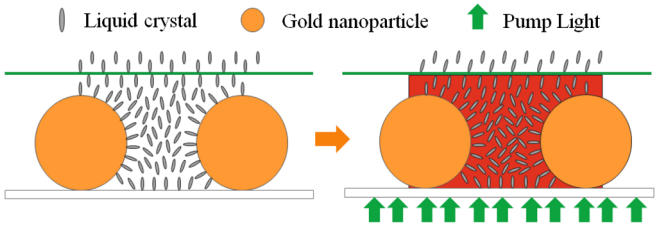


FIG. 3 (color online). Schematics illustrating LC molecular orientations in a LC-Au nanoparticle composite surface layer without (left) and with (right) a pump beam polarized along the surface. Orientations of LC molecules between Au nanoparticles are distorted by the pump field, reducing the anchoring strength of a LC at the effective surface marked by the green line. Above the green line, the bulk LC molecules orient uniformly, and if the SAE is finite, LC molecules at the surface will be tilted away from the surface normal by the field above the Fréedericksz transition.

We now focus on optical Fréedericksz transition (OFT) with $H = 0$. To check the dependence of the OFT threshold $I_{\text{th}}$ on the cell thickness $d$, predicted by Eq. (2), we measured $I_{\text{th}}$ of Au-LC and pure LC cells of various cell thicknesses with 2 h of Au nanoparticle deposition time. Figure 4(a) shows the results. With the 532-nm pump light, the observed decrease of $I_{\text{th}}$ with an increase of $d$ for both cells agree well with the prediction of Eq. (2) using $W_2(I)$ presented in Fig. 2(b). We notice that $I_{\text{th}}$ for the Au-LC cell is more than 1 order of magnitude smaller than that for the pure LC cell for all cell thicknesses.

To see how $W_2$ depends on the pump field enhanced by the local plasmon resonance around the Au nanoparticles, we measured $I_{\text{th}}$ versus $d$ with a 660-nm pump light for Au-LC cells of different cell thicknesses. The 660-nm beam was from a diode laser; unlike the 532-nm pump, its frequency is away from the peak of the plasmon resonance. The measured result is also presented in Fig. 4(a) in comparison with that of the 532-nm pump. It is seen that $I_{\text{th}}$ with the 532-nm pump is significantly lower at all $d$. This is due to the stronger local-field enhancement at 532 nm. We estimated the ratio of the local-field enhancements at 532 and 660 nm by assuming that the enhancement arises from individual 50-nm Au spherical particles imbedded in a medium with dielectric constants of $-5.2 + 2.3i$ and $-10 + 1.1i$ for 532 and 660 nm, respectively [26]. From the expression of the local field [27], we found the ratio to be 1.46, and accordingly the ratio of the local intensity enhancement at 532 and 660 nm is 2.1. We then expect $W_2(I_{660}) = W_2(2.1 \times I_{532})$. Knowing $W_2(I_{532})$ from Fig. 2(b) and hence $W_2(I_{660})$, we can obtain $I_{\text{th}}$(532 nm) and $I_{\text{th}}$(660 nm) versus cell thickness $d$ from Eq. (2). The calculated curves shown in Fig. 4(a) agree well with the measured data.

Higher surface density of Au nanoparticles on the windows of a LC cell, achieved by lengthening the Au

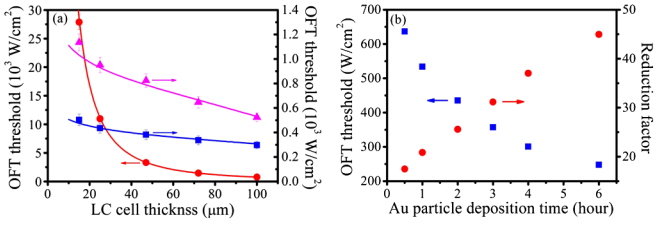


FIG. 4 (color online). (a) Thresholds of the OFT of Au-LC (blue squares) and pure LC (red circles) cells of various thickness pumped by a 532-nm beam, and the same Au-LC cells pumped by a 660-nm beam (magenta triangles). Lines are fits with Eq. (4). Typical error bars are shown. (b) OFT thresholds of Au-LC cells with various Au deposition times and the corresponding threshold reduction factors with respect to a pure LC reference cell; cell thickness is 25 $\mu$m.

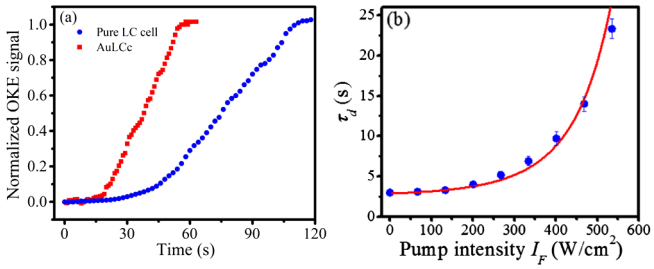


FIG. 5 (color online). (a) "Turn on" behavior of Au-LC (red squares) and pure LC (blue circles) cells; cell thickness is 47 $\mu$m. (b) Decay time $\tau_d$ of the Au-LC cell versus the final pump intensity $I_F$.

deposition time, reduces the SAE of the Au-LC cell more because more surface area is affected by local-field enhancement. This is seen from the measured $I_{\text{th}}$ for Au-LC cells prepared with different Au deposition times ranging from 0.5 to 6 h, depicted in Fig. 4(a). With a 0.5-h deposition time, $I_{\text{th}}$ compared with that of a pure LC cell is reduced by a factor of 17; with a 6-h deposition time, the reduction factor increases to 45.

Reduction of the SAE also sharpens the LC response to an orienting field [28] and speeds up the switch-on response of a LC cell [29]. The same effect was also observed with Au-LC cells. We measured the switch-on responses of Au-LC and pure LC cells of 47 $\mu$m thickness ($I_{\text{th}} = 380$ W/cm$^2$ and 3300 W/cm$^2$, respectively) by switching on a 532-nm pump beam to intensities 100 W/cm$^2$ above their respective $I_{\text{th}}$. The observed time dependences of the optical birefringence signal from the two LC cells are depicted in Fig. 5(a). The response time of the Au-LC cell is 50 sec and that of the pure cell is 110 sec. Weaker SAE is also known to lead to slower recovery time [30]. We measured the recovery time by monitoring the decay of the optical birefringence signal from a LC cell after the above-threshold pump intensity is suddenly reduced to a value of $I_F$ below threshold. The decay was found to be exponential with decay time constants $\tau_d$. In Fig. 5(b) we plotted $\tau_d$ versus $I_F$ for the 47 $\mu$m Au-LC cell. It is seen that $\tau_d$ increases with $I$ as $W_2(I)$ decreases. At $I_F = 0$, the observed $\tau_d = 3$ sec is the same as that of a pure LC cell of the same thickness. The model of Ref. [30] can be used to understand the observation. It predicts $\tau_d = \gamma d'^2/k_{33}\pi^2$ under finite $W_2$, where $\gamma$ is the viscosity coefficient, $d' = d + 2b$ is an effective cell thickness, and $b = k_{33}/W_2$. For our Au-LC cell, since $W_2$ changes with pump intensity $I$, we would expect $b = k_{33}/W_0 \exp(-I/I_{\text{sat}})$, but actually $b$ should further increase because the surface now refers to a thin layer composed of Au nanoparticles and disoriented LC molecules. We simply assume $b = k_{33}/W_0 \exp(-aI/I_{\text{sat}})$, with $a > 1$ as an adjustable parameter. As seen in Fig. 5(b), we can indeed use $\tau_d = \gamma d'^2/k_{33}\pi^2 2$ with $a = 1.42$ and $I_{\text{sat}} = 75$ W/cm$^2$ to fit the data well.

In conclusion, we have demonstrated that strong local-field enhancement from local plasmon resonance between Au nanoparticles can greatly change the effective surface anchoring strength of the LC and reduce the threshold of the Fréedericksz transition of a LC cell by 1 to 2 orders of magnitude. That a pump light can be employed to significantly reduce the switching field strength for LC reorientation and dynamically control the switching could provide many opportunities for future optoelectronic applications of a LC.

This work is supported in part by the National Natural Science Foundation of China (Grants No. 10874033, No. 60977047, No. 60907011, No. 61078052, and No. 11074051) and the National Basic Research Program of China (973 Program) (Grant No. 2011CB921802). We thank Professor Zongzhi Zhang and Professor Jing Li for the help with the measurements.

*leixu@fudan.ac.cn

[1] I. C. Khoo, J. Opt. Soc. Am. B **28**, A45 (2011).
[2] I. Janossy, A. D. Lloyd, and B. S. Wherrett, Mol. Cryst. Liq. Cryst. **179**, 1 (1990).
[3] I. Janossy and T. Kosa, Opt. Lett. **17**, 1183 (1992).
[4] T. V. Truong and Y. R. Shen, Phys. Rev. Lett. **99**, 187802 (2007).
[5] P. Yang, L. Y. Liu, L. Xu, and Y. R. Shen, Opt. Lett. **34**, 2252 (2009).
[6] S. T. Sun, W. M. Gibbons, and P. J. Shannon, Liq. Cryst. **12**, 869 (1992).
[7] O. Francescangeli, S. Slussarenko, and F. Simoni, Phys. Rev. Lett. **82**, 1855 (1999).
[8] E. Ouskova, Y. Reznikov, S. V. Shiyanovskii, L. Su, J. L. West, O. V. Kuksenok, O. Francescangeli, and F. Simoni, Phys. Rev. E **64**, 051709 (2001).
[9] B. Jerome, Rep. Prog. Phys. **54**, 391 (1991).
[10] H. Yokoyama, Mol. Cryst. Liq. Cryst. **165**, 265 (1988).
[11] L. M. Blinov, A. Y. Kabayenkov, and A. A. Sonin, Liq. Cryst. **5**, 645 (1989).
[12] S. Faetti, M. Gatti, V. Palleschi, and T. J. Sluckin, Phys. Rev. Lett. **55**, 1681 (1985).
[13] C. Rosenblatt, J. Phys. France **45**, 1087 (1984).
[14] R. B. Meyer, Appl. Phys. Lett. **12**, 281 (1968).
[15] J. J. Wysocki, J. Adams, and W. Haas, Phys. Rev. Lett. **20**, 1024 (1968).
[16] P. Pieranski, F. Brochard, and E. Guyon, J. Phys. France **34**, 35 (1973).
[17] A. J. Karn, S. M. Arakelian, Y. R. Shen, and H. L. Ong, Phys. Rev. Lett. **57**, 448 (1986).
[18] S. D. Durbin, S. M. D Arakelian and Y. R. Shen, Phys. Rev. Lett. **47**, 1411 (1981).
[19] H. L. Ong, Phys. Rev. A **33**, 3550 (1986).
[20] S. Xu, J. Shan, W. Shi, L. Y. Liu, and L. Xu, Opt. Express **19**, 12336 (2011).
[21] S. J. Barrow, A. M. Funston, D. E. Gomez, T. J. David and P. Mulvaney, Nano Lett. **11**, 4180 (2011).
[22] K. Skarp, S. Lagerwall, and B. Stebler, Mol. Cryst. Liq. Cryst. **60**, 215 (1980).
[23] A. M. Parshin and A. V. Barannik, Tech. Phys. Lett. **35**, 1166 (2009).

[24] See Supplemental Material at http://link.aps.org/supplemental/10.1103/PhysRevLett.109.147801 for surface anchoring energy change under various Au deposition times.
[25] L. T. Hung, S. Oka, M. Kimura, and T. Akahane, Jpn. J. Appl. Phys. **43**, L649 (2004).
[26] J. Jiang, K. Bosnick, M. Maillard, and L. Brus, J. Phys. Chem. B **107**, 9964 (2003).
[27] P. B. Johnson and R. W. Christy, Phys. Rev. B **6**, 4370 (1972).
[28] J. Nehring, A. R. Kmetz, and T. J. Scheffer, J. Appl. Phys. **47**, 850 (1976).
[29] G. P. Bryan-Brown, E. L. Wood and I. C. Sage, Nature (London) **399**, 338 (1999).
[30] X. Nie, R. Lu, H. Xianyu, T. X. Wu, and S. T. Wu, J. Appl. Phys. **101**, 103110 (2007).